1J2-1

High Frequency Thickness Expansion Mode Bulk Acoustic Wave Resonator Using LN Single Crystal Thin Plate

ニオブ酸リチウム単結晶薄板を用いた高周波厚み縦振動共振子

Kohei Matsumoto[1‡], Michio Kadota[1], and Shuji Tanaka[1] ([1]Grad. School of Eng., Tohoku Univ.)

松本　康平[1‡]，門田　道雄[1]，田中　秀治[1] ([1]東北大院　工)

1. Introduction

Surface acoustic wave (SAW) and film bulk acoustic wave (FBAW) filters are used for band selection from 700 MHz to 3.5 GHz. In recent years, the above frequency zone is extremely depleted with the spread of smartphones, and the 5th generation cellular network technology using 3.5 GHz or higher frequency bands has started. It is difficult to practically use the conventinal SAW devices in such high frequency because of the limit of microfabrication and increased resistance of an interdigital transducer (IDT). As a result, AlN and ScAlN BAW filters will be more widely used in the near future.

AlN and ScAlN are the major piezoelectric materals for BAW devices, while the use of $LiTaO_3$ (LT) and $LiNbO_3$ (LN) was investigated for better performance, e.g. wider bandwidth. For example, a 2.1 GHz film bulk acoustic resonator (FBAR) using a single crystal 45°Y-LN thin plate[1)], 3 GHz FBARs using CVD LN[2, 3)] and a 2.7 GHz FBAR using a single crystal X-LN thin plate[4)] were reported. However, the performances of those devices are not competitive against that of the existing FBAR. On the other hand, there are more design spaces for LN and LT FBARs. In this study, we investigated useful cut angles of rotated-Y LN for FBARs and fabricated and 800 MHz devices.

2. Simulation

The main modes of a BAW resonator include thickness shear (TS) mode and thickness expansion (TE) mode. In TS and TE modes, transverse and longitudinal waves propagate, respectively. The longitudinal wave has an about twice higher velocity than the transverse wave and suitable for high frequency devices.

Figs. 1 and 2 show the impedance ratio (Z ratio) and bandwidth (BW) of each mode in θ-rotated Y-LN calculated by FEM, respectively. Z ratio and BW are defined as

$Z\ \mathrm{ratio} = 20 \log\ Z_a/Z_r$　　1　and

$\mathrm{BW} = (f_a - f_r)/f_r \times 100\ (\%)$　　2 ,

where f_r and f_a are resonance and antiresonance frequency, and Z_r and Z_a are impedance at f_r and f_a, respectively. The FEM model assumes of a 250 μm thick air-suspended LN plate on both sides of which circle Al electrodes with a radius of 2 mm and a thickness of 1 μm are formed, which is a micromodel of FBAR.

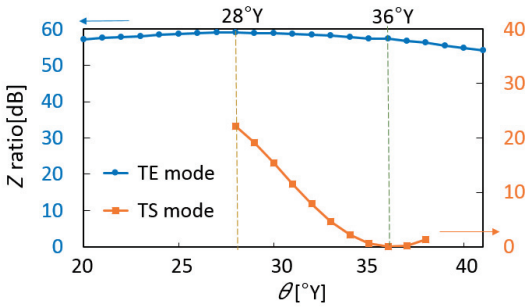

Fig. 1 Calculated relationship between impedance ratio and the rotated angle of Y-LN.

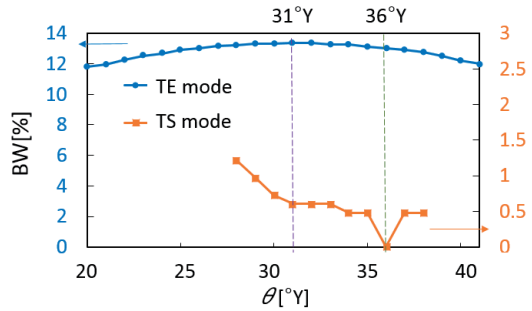

Fig. 2 Calculated relationship between bandwidth and the rotated angle of Y-LN.

28°Y-LN shows the highest impedance ratio for TE mode, but it also shows significant coupling to TS mode, which may generate a spurious response. On the other hand, 36°Y-LN has little coupling to TS mode as well as a large coupling to TE mode. In this study, therefore, 36°Y-LN was used to fabricate FBARs.

3. Fabrication

Fig. 3 shows the structure of the LN FBAR. We adopted the structure of the common electrode on the backside and the two hot electrodes on the front side, since it is difficult to access the electrode from the back side of the LN thin plate and fabricate one set of electrodes.

Email: matsumoto.kohei@mems.mech.tohoku.ac.jp

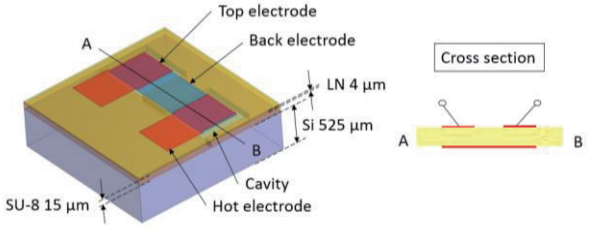

Fig. 3 Structure of LN FBAR.

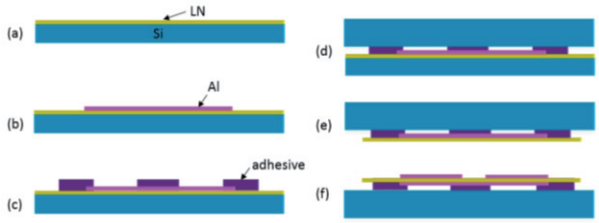

Fig. 4 Fabrication process of LN FBAR.

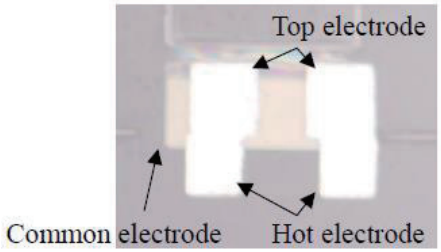

Fig. 5 Photograph of the fabricated LN FBAR.

The fabrication process of the FBAR is shown in Fig. 4. A LN substrate bonded to a Si substrate is polished to 4 μm thickness (a), and a common electrode made of Al is partially formed on the surface of the LN thin plate (b). Next, another Si substrate is bonded to the same side of LN via a 15 μm thick patterned photoresist (SU-8 3050, MICRO CHEM) (c), (d). The original Si bonded to LN is etched away (e), and two Al electrodes are formed on the newly exposed LN surface (f). Fig. 5 is the photograph of the fabricated FBAR.

4. Evaluation

Figs. 6 and 7 show the measured, fitted and simulated frequency characteristics, respectively. TE mode response is found at 800 MHz. Small responses at 450 and 970 MHz are derived from 0th and 1st TS modes, respectively. The TS mode responses are sufficiently small as predicted from Figs. 1 and 2. The main response has a BW of 10.3% and an Z ratio of 45 dB.

The equivalent circuit is shown in the inset of Fig. 7. The clamp capacitance C_0 may include a stray capacitance due to the electrodes structure. The resistance R_0 of 1.5 Ω is introduced to fit the antiresonance peak (i.e. Q_a) to the measured data. The resistance R_0 may be caused by the acoustic energy leakage at antiresonance related to the interconnection of two resonators.

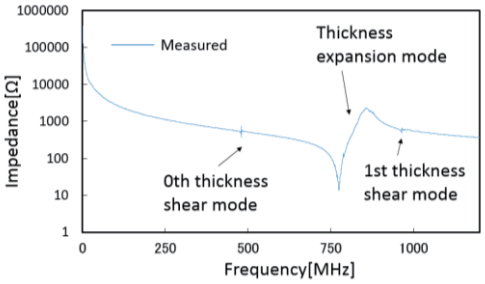

Fig. 6 Frequency characteristic of the fabricated LN FBAR.

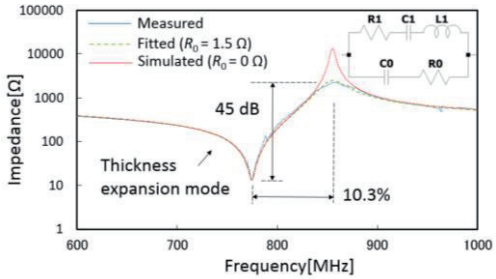

Fig. 7 Measured, fitted (R_0 = 1.5 Ω) and simulated (R_0 = 0 Ω) frequency characteristics.

It is considered that the performance can be improved by the optimization of the electrode structure and/or the interconnection of two resonators. It should be noted that the resonance frequency higher than 3 GHz is obtained by reducing LN thickness to 1 μm, which is feasible based on the past studies.

5. Conclusion

A TE mode FBAR was fabricated using 4 μm thick 36°Y-LN. The FBAR showed a BW of 10.3% and an Z ratio of 45 dB at 800 MHz. Spurious responses caused by TS modes are sufficiently small due to the selected cut angle. Q_a is not high probably because the effects of stray capacitance and routing resistance. We expect that a better performance is obtained by the optimization of the electrode structure.

Acknowledgment

We would like to express thanks to Dr. Hideki Takagi at National Institute of Advanced Industrial Science and Technology (AIST) for his support.

References

1. T. Tai, M. Sakai, Y. Osugi, K. Suzuki: Symp. Ultrason. Elect., **Vol. 28** (2007) p. 151.
2. M. Kadota, Y. Suzuki and Y. Ito: IEEE Int. Ultrason. Symp. 2010, p. 91.
3. M. Kadota, Y. Suzuki, Y. Ito: Jpn. J. Appl. Phys., **50** (2011) 07HD10.
4. A. Reinhardt, L. Benaissa, J. B. David, N. Lamard, V. Kovacova, N. Boudou, E. Defay: IEEE Int. Ultrason. Symp. 2014, p. 773.